# Dalton Transactions

Accepted Manuscript




This is an *Accepted Manuscript*, which has been through the Royal Society of Chemistry peer review process and has been accepted for publication.

*Accepted Manuscripts* are published online shortly after acceptance, before technical editing, formatting and proof reading. Using this free service, authors can make their results available to the community, in citable form, before we publish the edited article. We will replace this *Accepted Manuscript* with the edited and formatted *Advance Article* as soon as it is available.

You can find more information about *Accepted Manuscripts* in the Information for Authors.

Please note that technical editing may introduce minor changes to the text and/or graphics, which may alter content. The journal's standard Terms & Conditions and the Ethical guidelines still apply. In no event shall the Royal Society of Chemistry be held responsible for any errors or omissions in this *Accepted Manuscript* or any consequences arising from the use of any information it contains.



ROYAL SOCIETY OF CHEMISTRY

www.rsc.org/dalton

Dalton Transactions

ARTICLE

# Bidentate forms of β-triketimines: syntheses, characterization and outstanding performance of enamine-diimine cobalt complexes in isoprene polymerization†

Mohammed N. Alnajrani‡* and Francis S. Mair*

New cationic enamine-β-diimine cobalt complex [LCoBr.THF][BArF] (**I**) and its neutral analogue [$LCoBr_2$] (**II**) where L = [(2,4,6-$Me_3$-$C_6H_2$)NHCMe=C{CMe=(N-2,4,6-$Me_3$($C_6H_2$)}$_2$] and $BArF^-$ = [{3,5-$(CF_3)_2C_6H_3$}$_4$B]$^-$, were synthesised and then characterized by single-crystal X-ray diffraction, MALDI-MS, IR and elemental analysis. These complexes, the first examples reported where putatively tridentate β-triketimines prefer a bidentate coordination mode, were examined as catalysts for the polymerization of isoprene, activated by diethylaluminium chloride (DEAC) or ethylaluminium sesquichloride (EASC). The weakly coordinating BArF anion in **I** strongly improved activity in comparison to **II**. Both **I** and **II** produced polyisoprene of ca. 80% *cis*-1,4 and 20% 3,4 enchainment, with trace levels of *trans*-1,4 and no 1, 2 polymer. A kinetic study for both **I** and **II** demonstrated that the polymerization was first-order in monomer and that approximately 46% and 50% of cobalt formed active centres for **I** and **II** respectively. EASC was the most active of a range of organoaluminium compounds screened for both **I** and **II**. The resulting activities of up to $6 \times 10^5$ mol isoprene $mol^{-1}$ Co $h^{-1}$ are the highest yet recorded for catalysts selective for *cis*-1,4 enchained polyisoprene.

## Introduction

The stereospecific polymerization of 1,3-diene monomers has posed an interesting challenge for many academic and industrial research groups because of the numerous applications of polydienes in the rubber industry, and the many possible pathways that polymerization of dienes can take.[1] Currently, transition metal and lanthanide complexes are used in the polymerization of 1,3-dienes. A series of different catalytic systems have been found to be efficient in controlling the microstructure of the produced polymers.[1-5] Industrially, catalysts based on Nd are the most preferred where a very high level of *cis*-1,4 selectivity in the polymerization is desired.[6] A summary of the development of the various heterogeneous and homogeneous (ligated) metal catalysts, which can select for high *cis*-1,4, high *trans*-1,4, high 3,4- syndiotactic, *alt cis*-1,4/3,4, and other less regular microstructures, can be found in our previous paper in this series.[7] Most pertinent here are the results showing the control on activity and microstructure achievable by catalyst systems based on metal complexes with ligands having donor atoms such as nitrogen, oxygen and phosphorus.[8-12] Ligands coordinated to the metal have been found to affect both the activity and the form (*syn* or *anti*) of the allyl active centre during the polymerization.[13]

These effects can be modified by changing the steric and electronic properties of the ligands.[14-16] Recently, cobalt catalysts have received more interest in the polymerization of 1,3-dienes, due to the lower cost and better availability of Co versus Nd.[17] Several papers reported the influence of ligands in controlling the performance of cobalt complexes.[14, 18-20] These complexes mainly employed *bis*-imino-pyridine and analogous cases such as *bis*-benzimidazolylpyridine, exclusively planar *mer*- *N,N,N*-ligands on cobalt. In contrast, in our previous work on Cr(0), Mo(0), W(0),[21] Tl(I),[22] Ni(II)[23] and Co(II)[7, 24], the triketimine *N,N,N* ligands were found exclusively to bind in a *fac* tridentate manner. In our mechanistic hypotheses, we reasoned on the basis of electron counts that it was likely that bidentate forms may be found at key points in the catalytic cycle. In such forms, the change in coordination would be accompanied by a CH/NH tautomerization, to generate bidentate enamine-diimine forms of the putatively tridentate β-triketimines. Here, we report the first examples of such bidentate forms in fully characterized solid compounds, and demonstrate that not only are they catalytically competent, but also that they are significantly more active than their tridentate counterparts, placing them as the most active of all metal complexes thus far found to produce predominantly *cis*-1,4 polymer, surpassing even the best examples from the lanthanides in terms of activity. Thus, they offer hope that synthetic polyisoprene might be accessed even in the event of increase in the demand for lanthanides for their magnetic properties in energy generation.[25]

*School of Chemistry, The University of Manchester, Chemistry Building, Manchester, M13 9PL, UK. E-mail: mair@manchester.ac.uk*
† Electronic supplementary information (ESA) available.
‡Current address: King Abdulaziz City for Science and Technology, Kingdom of Saudi Arabia, PO Box 6086, Riyadh 11442. E-mail: mnajrani@kacst.edu.sa

Dalton Transactions Accepted Manuscript

## Results and discussion

### Synthesis and characterization of enamine-diimine cobalt complexes

A cationic enamine-diimine cobalt complex **I** was synthesized from the reaction of the enamine-diimine ligand (L) with cobalt bromide in the presence of NaBArF (Scheme 1). The reaction was firstly carried out in THF, which was then removed in *vacuo* and replaced with DCM, before layering with hexane. Green crystals of **I** were formed in good yield. These were then characterized by single crystal X-ray diffraction. The crystal and molecular structure of **I** is shown in Figure 1, with key structural data recorded in Table 1. It became apparent that the removal of THF was incomplete; one molecule of THF is retained in the coordination sphere of the Co(II) in **I**. In the several previous examples of reaction of enamine-diimines with Co(II) and other metals, in all cases the ligands converted exclusively to the tridentate β-triketimine forms.[7, 21-24] Here, uniquely, the enamine-diimine tautomer present in the proligand is retained, though the internal hydrogen bond is lost. This different behaviour may be ascribed to the presence of alkyl substituents in both *ortho* positions of each aryl, a degree of bulk which appears not be tolerated in the tridentate form. However, it must be a fine balance, since the same ligand is reported to bind in a tridentate fashion to Ni(II), also with BArF counterion,[23] forming a bromide-bridged dimer closely analogous to the previous known Co(II) dimers.[7, 24] Given that the radius of 5-coordinate Ni(II) is *smaller* than that of Co(II) by 0.04 Å,[26] this seems surprising, and is suggestive that steric factors alone do not explain the phenomenon. However, essentially the same ligand geometry is found when the reaction is repeated in the absence of THF and of BArF (scheme 1) yielding the neutral **II**, which was recrystallized from orthodichlorobenze to give green crystals suitable for diffraction. The crystal and molecular structure of **II** is shown in Figure 2, with structural data tabulated alongside those of **I** in Table 1.

The geometry of the four coordinate cobalt atom was found in both **I** and **II** to be deformed tetrahedral. In **I** the bidentate N,N'-L, one bromine atom and a coordinated THF oxygen (Figure 1) form the Co(II) coordination sphere. This $N_2OBr$ ligation environment is novel for Co. In **II**, two bromine atoms and two nitrogen atoms from the ligand provide the coordination shell of Co(II). There are many tetrahedral $N_2CoX_2$ complexes[27-29] (X = Br or Cl); the one most similar to **II**, and **I**, is the diimine complex $[H_2C(MeC=(N\text{-}2,6\text{-}Me_2(C_6H_3))_2]CoBr_2$.[30] The Co-N and Co-Br bond lengths and angles of **I** and **II** are generally similar to the values in the diimine complex.[30] Comparing the neutral enamine-diimine cobalt complex **II** with the cationic complex **I**, the bonds length of Co-N and Co-Br were found to be marginally but consistently longer (Table 1), a fact ascribable to the reduced electron-electron repulsion in **I** with respect to **II**, a result of the cationic charge and the replacement of a large and soft bromide ligand with a smaller, harder THF oxygen. The six-membered ring of the central carbon of the diimine, [Co-N1-C2-C3-C4-N2] in both **I** and **II** adopted a boat conformation, as in $[H_2C(CMe=(N\text{-}2,6\text{-}Me_2(C_6H_3))_2CoBr_2]$ and in all other complexes of neutral β-diimines.[31, 32] The N1-Co-N2 angles in **I**, **II** and $[H_2C(MeC=(N\text{-}2,6\text{-}Me_2(C_6H_3))_2]CoBr_2$[30] were closely similar at 94.49(13)°, 93.06(12)° and 95.3(2)° respectively. The opposing angles were closer to the regular tetrahedral angle of 109.5°; where the Br-Co-O angle of **I** was 107.28(10)°, the Br-Co-Br angles of **II** and $[H_2C(MeC=(N\text{-}2,6\text{-}Me_2(C_6H_3))_2]CoBr_2$ were 108.97(3)° and 110.62(3)° respectively.

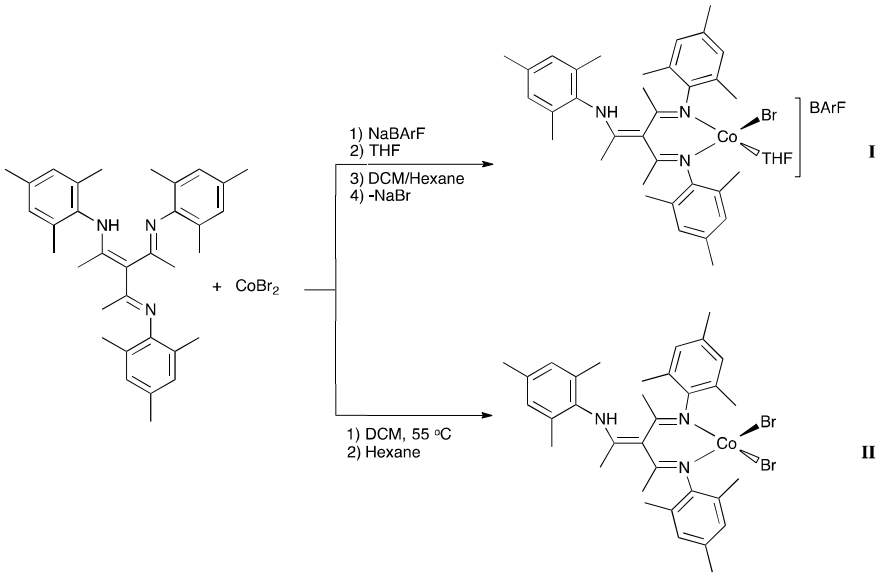


Scheme 1 Synthesis of **I** and **II**.

Dalton Transactions Accepted Manuscript


This journal is © The Royal Society of Chemistry

Hence, the coordination tetrahedra were only moderately distorted. The terminal Co-Br bonds in all three examples were shorter (range: 2.31-2.38 Å) than the distances of 2.5 Å seen in the analogous β-triketimine dimers,[7, 24] since in the dimers the bromides were bridging. Furthermore, the 5-coordinate metal ion in the dimers would be expected to exhibit larger bond lengths than those to be found in an otherwise similar 4-coordinate complex. The Co-O bond to THF in **I** was at 1.992(3) Å typical of similar four-coordinate examples such as 1.989(3) Å in $CoBr_2$(2,5-dimesitylpyridine)(THF).[33]

The C=N str was observed at 1653 $cm^{-1}$ in the Infra-Red spectrum of the free ligand, but was shifted to 1610 $cm^{-1}$ as it coordinated to cobalt in **I**. This shift is ascribed to strong donation from C=N to Co(II). In **II**, the red-shift was smaller (C=N str 1628 $cm^{-1}$). In **I** a greater degree of donation of C=N bonding density to cobalt is evidenced in the slight weakening of the C=N bond with respect to that in **II**. This is due to replacement of an effective σ-donor bromide anion in **II** by a small, hard, electronegative but neutral oxygen donor in **I**. Hence, the pull of the Co(II) on the electron-density from the imine ligand is commensurately greater in **I** than in **II**. Consequently, a shorter Co-N bond is correlated with a longer C=N bond (Table 1). In the free ligand Infra-Red spectrum, NH was not resolved, being broadened and dropped in frequency by the internal hydrogen bond [21, 23] while for the complexes **I** and **II** it appeared at 3375 $cm^{-1}$ and 3411 $cm^{-1}$ respectively, confirming the presence of the enamine group.

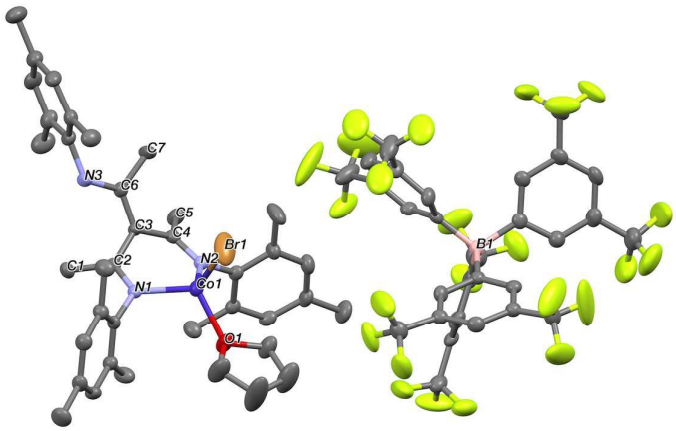


**Figure 1** Structure of **I** with all hydrogen atoms omitted.

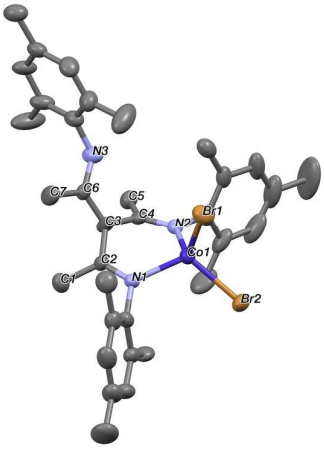


**Figure 2** Structure of **II** with all hydrogen atoms omitted.

**Table 1** Selected bond angles [°] and lengths [Å] of **I** and **II**.

| **I** | | **II** | |
|---|---|---|---|
| Co-N1 | 1.979(3) | Co-N1 | 2.019(3) |
| Co-N2 | 1.977(3) | Co-N2 | 2.017(3) |
| Co-Br | 2.3153(7) | Co-Br1 | 2.3690(7) |
| Co-O | 1.992(3) | Co-Br2 | 2.3808(7) |
| N1-C2 | 1.293(4) | N1-C2 | 1.279(5) |
| N2-C4 | 1.286(5) | N2-C4 | 1.283(5) |
| N3-C6 | 1.351(5) | N3-C6 | 1.330(5) |
| N1-Co-N2 | 94.49(13) | N1-Co-N2 | 93.06(12) |
| Br-Co-O | 107.28(10) | Br1-Co-Br2 | 108.97(3) |

**Isoprene Polymerization**

**Initiation and possible mechanistic pathways**

The polymerization of isoprene by enamine-diimine cobalt complexes was carried out in chlorobenzene using diethylaluminium chloride (DEAC) or ethylaluminium sesquichloride (EASC) as co-catalyst. It is proposed, given the essentially identical selectivities in polymerization (*vide infra*), that both **I** and **II** have the same cationic active centre (Scheme 2). The organoaluminium reagent (DEAC or EASC) plays several roles, and is present in large excess. Firstly, in the case of **I**, it acts as a Lewis acid in stripping the THF from cobalt. Secondly, for both **I** and **II**, it alkylates the cobalt in a metathesis reaction. Thirdly for **II**, it again acts as a Lewis Acid to strip ligands from Co to form weakly coordinating anions $\mathbf{X}^-$. There are a variety of possible identities for these, including $[Et_2AlClBr]^-$, $[Et_2AlCl_2]^-$, $[EtAlCl_3]^-$, $[Et_3AlCl]^-$, etc., which will subsequently be termed '$[Al]^-$'.

For **I**, no such step is necessary since it is already furnished with the weakly coordinating anion BArF. Such a sequence would result in either case **I** or **II** with putative active centre **Z** (Scheme 2). A further feature of **Z** to be expected, given the large excess of the aluminium reagent and the presence of an un-coordinated enamine in both **I** and **II**, is coordination of a further equivalent of Lewis acid to the basic nitrogen of the enamine. In so doing, it is closely analogous to the organoaluminium-activated α-keto-β-diimine complexes of Ni(II) reported by Bazan and co-workers as active in ethylene polymerization.[34] However, distinct from that case is the possibility here via NH acidity of further reaction by alkane elimination to form an aza-allyl aluminium complex such as **Z***. Examples of such complexes show both σ and π-coordination.[35] There are several possible pathways from this point to polymer, with the particular one chosen being a function of the relative activation energies of each step.[36-38]

Dalton Transactions Accepted Manuscript

Restricting cases firstly to those where 1,4-enchainment of monomers results, the possible paths from either s-*trans* or s-*cis* coordinated monomer are shown in Scheme 3. The routes taken are recorded in the microstructure of the resultant polymers, which varied with temperature and with co-catalyst ratio in intriguing ways that may shed further light on mechanistic details.

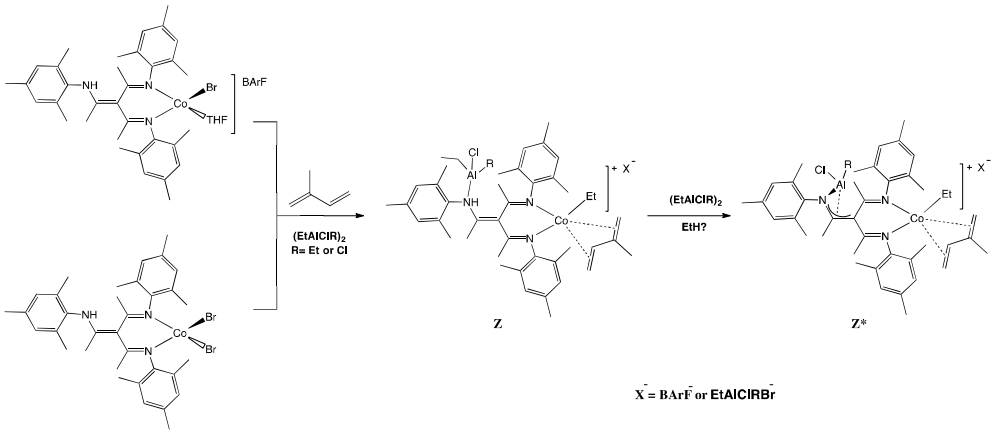


**Scheme 2** Formation of active centres from **I** and **II** by reaction with aluminium alkyls.

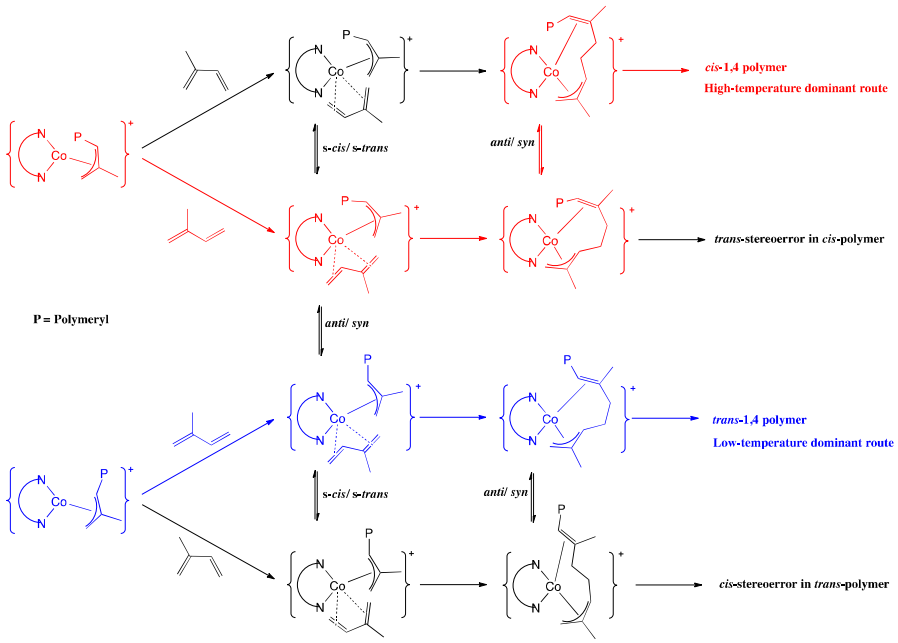


**Scheme 3** Possible Polymerization routes resulting in *cis* or *trans* enchainment of isoprene.

## Kinetic Study

The first point probed was the rate-time profile of the reaction. Several runs were terminated at different timepoints. The results, in terms of activities, molecular weights and polymer microstructures are presented in Table 2. Firstly, there was no change in stereoselectivity with time. Secondly, it was noted that virtually complete conversion was possible in less than 1 hour. Finally, much can be deduced from a careful analysis of the progression of productivity over time. A plot of $\ln([IP]_0/[IP]_t)$ against polymerization time, where $[IP]_0$ is the initial isoprene monomer concentration and $[IP]_t$ is isoprene monomer concentration at time $t$, gave a linear relationship: the polymerization of isoprene by both **I** and **II** were first-order with respect to monomer (see supplementary information for plots). Therefore, the polymerization rate depends on isoprene concentration as shown in equation (1), where $k = k_p[C^*]$, where $k_p$ is the rate constant of propagation, $[C^*]$ is the concentration of active centres and [IP] is the concentration of isoprene monomer.

Dalton Transactions Accepted Manuscript


This journal is © The Royal Society of Chemistry

**Table 2** The polymerization of isoprene by **I** and **II**.

| Complex | Time | Conversion (%) | $M_w$ [b] (g mol$^{-1}$) ×10$^5$ | $M_n$ [b] (g mol$^{-1}$) ×10$^5$ | $Đ$ [b] | Microstructure[c] (%) | | | |
|---|---|---|---|---|---|---|---|---|---|
| | | | | | | *Cis*-1,4 | *Trans*-1,4 | 1,2 | 3,4 |
| **I** | 0 | - | - | - | - | | | | |
| | 5 min | 29.4 | 2.6 | 1.4 | 1.86 | | | | |
| | 10 min | 52.9 | 2.9 | 1.5 | 1.93 | | | | |
| | 15 min | 62.7 | 3.2 | 1.6 | 2.00 | 78.2 | 0.2 | 0 | 21.6 |
| | 20 min | 76.0 | 3.8 | 1.7 | 2.24 | | | | |
| | 35 min | 89.1 | 4.8 | 2.0 | 2.40 | | | | |
| | 45 min | 98.1 | 5.1 | 2.1 | 2.43 | | | | |
| **II** | 0 | - | - | - | - | | | | |
| | 1 h | 19.0 | 1.9 | 0.8 | 2.38 | | | | |
| | 4 h | 46.0 | 2.3 | 0.9 | 2.56 | | | | |
| | 6 h | 64.0 | 2.4 | 0.9 | 2.67 | 79.3 | 0.2 | 0 | 20.5 |
| | 12 h | 91.0 | 3.1 | 1.0 | 3.10 | | | | |
| | 18 h | 94.1 | 4.9 | 1.5 | 3.27 | | | | |

[a] Conditions: Catalyst: 5 µmol; co-catalyst: DEAC; Al/Co:150; Isoprene: 5 mL solvent: 30 mL chlorobenzene; T:35 °C. [b] Determined by GPC. [c] Determined by $^{13}$C NMR.

The value of $k$ can be calculated as the gradient of the line.

$$-\frac{\mathrm{d[IP]}}{\mathrm{d}t} = k[\mathrm{IP}] \quad (1)$$

In the case of **I**, $k$ was found to be $1.29 \times 10^{-3}$ s$^{-1}$ which means that the value of propagation rate ($R_p$) is $1.84 \times 10^{-3}$ M s$^{-1}$. In the case of **II**, the value of $k$ was found to be 0.17 h$^{-1}$ ($\approx 4.7 \times 10^{-5}$ s$^{-1}$) leading to a value of $R_p$ of $6.75 \times 10^{-5}$ M s$^{-1}$. Consequently, the catalytic activity of **I** was much higher than that of **II**. This phenomenon may be ascribed to the interaction of the counter-ion with the cationic active centre. In the case of **I**, it is well-known that the BArF$^-$ anion is a very weakly coordinating and large counter-ion,[42] so any ion-pairing between BArF and the cobalt cation in chlorobenzene would be loose, facilitative of fast insertion of incoming monomers. In the case of **II**, the contact ion pair formed between cobalt cation and [Al]$^-$ anion depends strongly on the type of Al anion. As discussed previously, there are several possible Al anions, all of them likely to form tighter ion pairs than BArF, via bridging chlorides. A series of contact/non-contact ion pair equilibria would precede the monomer coordination equilibria, with [Al]$^-$ partially blocking the coordination site for monomer, or preventing close approach of chain end to coordinated monomer, thus inhibiting propagation. Such counterion effect are well-known from metallocene catalysis of ethylene polymerization,[39] and have also been seen, though with less-stark variation, in isoprene polymerization.[40] As a result, the propagation rate for **I** is significantly higher than that for **II**.

Comparing the activity of bidentately coordinated **I** to the tridentately coordinated β-triketimine cobalt complexes published previously,[7] it was found that **I** was substantially more active than these complexes, a monomeric form of which is shown as **III** below, even though they shared with **I** the BArF counterion.

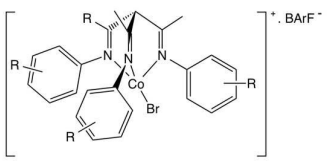


**III**

In the case of **III**, it was proposed that the coordinated ligand became bidentate as the complex was dissolved and then activated by alkylation reagent before inserting the first monomer. Therefore, the final form of active centre postulated is closely analogous to that shown in Scheme 2, though it has a more circuitous route to traverse before finding this form, and the aryl substituents would be different. Experimentally, the activity of **I**, when activated with DEAC under standardised conditions, was much higher ($R_p = 1.84 \times 10^{-3}$ M s$^{-1}$) than that previously recorded for **III** ($R_p = 1.1 \times 10^{-4}$ M s$^{-1}$). There appear to be two factors behind this difference. The first concerns the proportion of cobalt which forms active centres (C*). The value of [C*] was estimated by extrapolating back the variation in the number of chains to zero conversion, after the method of Boucher *et al.*[41] In the case of **III**, this was *ca.* 12%, whereas for **I** it was 46%; an approximately fourfold greater ratio of the cobalt present was active in **I** (supplementary information). The tridentately coordinated β-triketimine form **III** is a dormant pro-catalyst, in equilibrium with a bidentate active form. In **I** this equilibrium is pre-saturated in favour of the active form. However, the superior activity of **I** over **III** is only partly explained by a greater proportion of active sites. The propagation at each site must

Dalton Transactions Accepted Manuscript

also be faster in order to explain the observed activities. This is a function of the steric and electronic effects of the aryl substituents, which were bulkier in **I** than in most examples of **III**. Increased bulk might promote activity by weakening the binding between allyl chain end and Co(II), in a manner similar to that which operates to maximise activity of Ni(II) in ethylene polymerization.[42]

Consistent with the greater number of active sites, $M_w$ produced by **I** was 61.1 % ± 4.9 of the value of $M_w$ produced by **III** with the same yield. The molecular weight of the polymer produced by **I** increased linearly with the polymerization time, from 2.6 × $10^5$ g $mol^{-1}$ after 5 minutes to 5.1 × $10^5$ g $mol^{-1}$ after 45 minutes, but the trendline did not pass through the origin. Hence, we do not claim a living polymerization here, since there was an increase in the value of dispersity as time progressed due to chain transfers, firstly to monomer (at low conversion where the monomer was plentiful) and then to polymer (at high conversion as monomer dwindled but polymerised alkene groups became abundant).[43] In general, values of dispersity hovered around those expected of a most-probable distribution (2), though on occasion were greater than this. In the case of **II**, the molecular weight increased slowly for the first 12 hours, reaching a value of 3.2 × $10^5$ g $mol^{-1}$ at 91.0% conversion with dispersity of 3.10. When the polymerization was left for a further six hours there was a jump in the values of $M_w$ and $M_n$ due to the presence of chain transfer to polymer resulting in crosslinking. A treatment of the data similar to that used for **I** resulted in a value of 50% of cobalt in active sites in **II**. This was similar to the value found for **I**, in fact slightly higher. Despite this fact, **II** was less-active ($R_p$ = 6.75 x $10^{-5}$ M $s^{-1}$), showing that the closer contact of $[Al]^-$ relative to $BArF^-$ somewhat impeded propagation.

Turning to molecular weight distributions, these had an interesting time-dependent variation. In general, for **I**, there was a small low-molecular weight tail, but crosslinking broadened the distribution after most monomer had been consumed. Figure 3 shows the Gel Permeation Chromatograms of polymer samples prepared using **I**/DEAC at 5 min (29% conversion), 45 min (98% conversion) and 120 min (100% conversion). There is little change with the low molecular weight tail, but the growth of the high-molecular weight fraction at high conversion, due to chain transfer to polymer, is clear.

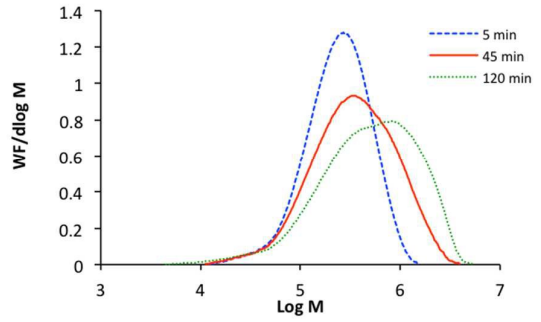


**Figure 3** GPC curves of Polyisoprene by **I**/DEAC; for 5, 45 and 120 minutes.

**Influence of polymerization temperature**

The produced polymer was characterized in all cases by NMR in order to investigate its microstructure. This was not influenced by the nature of counter-ion above room temperature. The polyisoprene contained a mixture of *cis*-1,4, *trans*-1,4 and 3,4-enchained monomers. For example, at 35 °C, with DEAC co-catalyst at Co:Al ratio 150, the polymer produced by **I** was 78.2% *cis*-1,4, 0.2% *trans*-1,4 and 21.6% 3,4, while the polymer produced by **II** was 79.3% *cis*-1,4, 0.2% *trans*-1,4 and 20.5% 3,4. Broadly similar degrees of selectivity were obtained by **I** and **II** operating under the same conditions, as might be expected if the active site **Z** or **Z*** is the same in either case, differing only in the identity of the counterion $X^-$ (Scheme 2). The selectivity changed only modestly over a range of temperatures, excepting the low-temperature run of **I**. Consultation of Scheme 3 shows how the *cis*-1,4 structure can be obtained, either from $\eta^4$ coordination of s-*trans* isoprene, and subsequent s-*cis*/s-*trans* isomerization of the coordinated diene, or *syn/anti* isomerization of the allyl produced by addition of the chain end to the diene. The stereochemistry of enchainment of the penultimate diene in the chain is determined at this point. The results of an examination of the temperature dependence of activity and stereoselectivity in isoprene polymerization for **I** and **II** are presented in Table 3 and give clues as to the pathways chosen by these catalysts.

The activities vs temperature are shown as bar charts in figures 18 and 20 on pages 15-16 of the supplemental data. It is clear from these figures that there is a drop in activity at higher temperatures, which is evidence of active site death, in addition to a drop in isoprene solubility at elevated temperature.[11,44] We show *vide infra* that the polymerization temperature had an influence also on the number of active sites, as was supported by GPC results as presented in page 10 figure 4 and in more detail in the supporting information. In addition, we further show that the active site allyl form (*syn* or *anti*) was strongly affected by the temperature; Therefore, the rates of the polymerization at various temperatures are influenced by several factors, such as the form of allyl active sites, and the number of active sites, rather than the single factor inherent in the assumptions behind the graphical method of determination of activation energy. It is for this reason that we show in figures 18 and 20 (supplemental) only bar charts versus temperature, rather than attempt to further interpret the data graphically to extract activation energies. There does, however, appear to be an approximately exponential rise in activity with temperature as predicted by Arrhenius kinetic laws, but only below 70 °C, before extensive catalyst deactivation blurs the trend.

More interestingly, there are strong effects on selectivity for **I**, but less-so for **II**. For **I**, *trans*-enchainment is greatest at low temperatures. This suggests that addition from *syn*-allyl chain end, derived from addition to an s-*trans*-bound monomer, with neither the allyl nor the bound monomer attaining sufficient energy to isomerise, is the favoured low-temperature route, shown in blue in Scheme 3. This in turn suggests that s-*trans*-coordination of isoprene is most favoured. This is consistent

Dalton Transactions Accepted Manuscript


This journal is © The Royal Society of Chemistry

with the observations and computations of others with iron and lanthanide systems.[36-38] How, then, does *cis*-enchained polymer come to dominate? This is due to the fact that *syn*-allyl (derived by addition of chain end to *trans*-coordinated monomer) is more stable, and hence less reactive, also borne out computationally in other systems.[36-38] In addition, *syn/anti* isomerization of allyls is known to be facile, especially when promoted by additional Lewis bases.[45] Hence formation of *anti*-allyl by isomerization leads to a more reactive chain end which leads *cis*-enchainment to dominate in the product distribution at higher temperatures for **I**, even though it may be a minor component of the forms in solution. This in turn is because of the activation energy of the *syn/anti* allyl isomerization is sufficiently high for **I** that only a small fraction of sites attain it at 0 °C, but progressively greater proportions of sites can isomerize to the more reactive *anti*-allyl as temperatures increase, hence it dominates in the product. This is shown as the high-temperature favoured route (red) in Scheme 2. As temperature climbs higher, then as is generally expected, other pathways become activated, and selectivity drops somewhat. Another fact supporting this view is that the activity is low when there are few *anti*-allyl ends (due to the low reactivity of *syn*-allyl units), and becomes progressively higher as the *syn/anti* isomerization becomes activated. This hypothesis can also fit the data for **II**, despite the fact that a much weaker temperature dependence of selectivity was noted. The data fits if it is assumed that the activation energy for *syn/anti* allyl isomerization is lowered by the presence of $[Al]^-$, hence a greater proportion of the more reactive *anti* chain ends is present for **II** even at low temperatures. A suggested mechanism for the catalytic effect of $[Al]^-$ on *syn/anti* isomerization is shown in Scheme 4. In short, coordination of the anion to Co(II) via a bridging halide could trigger $\eta^3$-$\eta^1$ hapticity change in the allyl, thus facilitating isomerization. However, the same type of anion coordination may also impede addition of allyl to monomer, or perhaps even coordination of monomer, thus explaining why **I** is so much higher in activity than **II**.

This satisfactorily explains the varying nature of temperature-dependence of *cis/trans* 1,4 enchainment of monomer in **I** and **II**. What remains is to explain the approximately 20% frequency of 3,4 enchainments in both cases. As has been pointed out by others,[13] and as discussed by us in our previous paper[7] this would be expected of $\eta^2$-3,4 coordinated monomer. This *ca*. 20% 3,4-enchainment feature is shared by other nitrogen-ligated cobalt catalysts,[20] though cobalt carboxylate complexes give less than 50% *cis*-1,4 polymer,[46] and cobalt phosphines can give exactly 50% *cis*-1,4/3,4 alternating polymer.[47] The 20% levels of 3,4-enchained monomers found for both our tridentate trisketimines[7] and bidentate enamine-diimines **I** and **II** are similar to eachother, further supporting the idea that active forms are bidentate in all cases. Such levels of 1,4-*cis* selectivity do not compete with those attained with lanthanide catalysts, approaching 96% in some cases,[40] and even higher in some less-active cases,[48] but can exceed the best lanthanide systems in activity (*vide infra*) and do provide the opportunity for lower-temperature non-sulfur-promoted crosslinking, which could offer advantage in some applications.[49, 50] Steric compression in **I** and **II**, as for our triketimine examples[7] resulted in the absence of 1,2-enchained monomer. Furthermore, by careful analysis of $^{13}$C NMR spectra it was noted that 4,1 regioerrors followed 3,4 errors to a disproportionate extent, suggesting that the chain end resulting from 3,4 addition is less-selective than the normal allyl chain end. This might point to the importance of coordination of previously enchained monomer as a stabilizing influence on the active site (see Scheme 2). Other distributions of stereo- or regio-errors were statistical in nature, as in the previously reported examples.[7]

The $M_n$ was strongly affected by the polymerization temperature. For **I**, $M_n$ increased with temperature to an optimum value of $1.8 \times 10^5$ g mol$^{-1}$ at 35 °C; further increase of temperature resulted in a reduction of $M_n$ ($8.0 \times 10^4$ g mol$^{-1}$ at 100 °C). In the case of **II**, the optimum value of $M_n$ was $1.9 \times 10^5$ g mol$^{-1}$ at 0 °C before it started decreasing with increase of temperature; the lowest value was $4.0 \times 10^4$ g mol$^{-1}$ at 100 °C. In comparison to other cases, these are relatively high molecular weights. The drop in $M_n$ with temperature was due to increases in the rate of chain transfers. At elevated temperature for both **I** and **II**, as for **III**[7] dispersity increased. This was due to the combined effects of chain transfer and catalyst deactivation reactions.[14, 24] The growth of low-molecular weight fractions is clear from the GPC data shown in Figure 4. The general drop in the maximum of the main peak is rationalised by acceleration of chain transfer to monomer or aluminium, but the relative growth of the low molecular weight shoulder is possibly evidence of increasing contribution of a different reactive site, perhaps **Z***, at higher temperatures. Further information on these issues is presented as supplementary material.

**Table 3** Effect of temperature on the polymerization of isoprene. [a]

| Complex | Time (min) | T (°C) | Conversion (%) | $M_w$ [b] (g mol$^{-1}$) $\times 10^5$ | $M_n$ [b] (g mol$^{-1}$) $\times 10^5$ | $Đ$ [b] | Microstructure [c] (%) | | | |
|---|---|---|---|---|---|---|---|---|---|---|
| | | | | | | | *Cis*-1,4 | *Trans*-1,4 | 1,2 | 3,4 |
| **I** | 20 | 0 | 1.0 | 0.7 | 0.6 | 1.17 | 42.2 | 43.0 | 0 | 14.8 |
| | 20 | 20 | 3.0 | 2.0 | 1.3 | 1.54 | 73.4 | 6.1 | 0 | 19.5 |
| | 20 | 35 | 76.0 | 3.8 | 1.8 | 2.11 | 78.2 | 0.2 | 0 | 21.6 |
| | 20 | 70 | 100 | 3.3 | 1.0 | 3.30 | 77.3 | 0 | 0 | 22.7 |
| | 20 | 100 | 59.7 | 1.8 | 0.8 | 2.25 | 75.0 | 0 | 0 | 25.0 |
| **II** | 360 | 0 | 4.4 | 3.8 | 1.9 | 2.00 | 78.3 | 1.4 | 0 | 20.3 |
| | 360 | 20 | 30.0 | 2.2 | 1.0 | 2.20 | 80.2 | 0.5 | 0 | 19.3 |

Dalton Transactions Accepted Manuscript

| | | | | | | | | | |
|---|---|---|---|---|---|---|---|---|---|
| 360 | 35 | 64.7 | 2.3 | 0.8 | 2.88 | 79.8 | 0.2 | 0 | 20.0 |
| 360 | 70 | 92.4 | 1.7 | 0.5 | 3.40 | 78.7 | 0.1 | 0 | 21.2 |
| 360 | 100 | 61.8 | 1.0 | 0.4 | 2.50 | 76.5 | 0.2 | 0 | 23.3 |

[a] Conditions: Catalyst: 5 µmol; co-catalyst: DEAC; Al/Co:150; isoprene: 5mL; solvent: 30 mL chlorobenzene. [b] Determined by GPC. [c] Determined by $^{13}$C NMR.

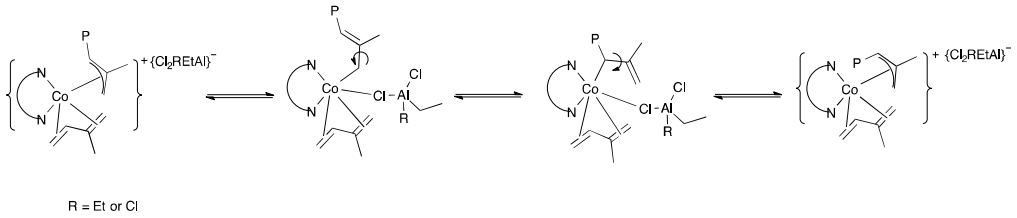


**Scheme 4** Aluminium-ion promoted *syn/anti* isomerization in **II**.

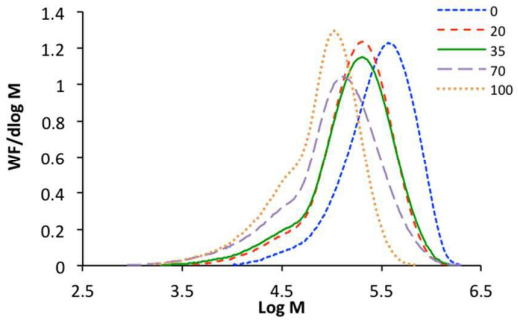


**Figure 4** GPC curves of polyisoprene produced by **II**/DEAC at different temperatures.

### Influences of co-catalyst and [Al]/[Co] mol ratio

In order to further investigate chain transfers to Al, a series of polymerizations were carried out with different Al:Co mol ratios. The results are summarized in Table 4. In the case of **I**, there was a linear relationship between $M_n$ and [Al] over the range of Al:Co mol ratio from 25 to 150 ($r^2 = 0.98$). This is in stark contrast to group 4[51] and lanthanide examples[52-54] when $M_n$ *decreased* with increasing Al. In addition, the activity of **I** increased with Al:Co mole ratio, as did the number of chains ($N_c$) (fit to linearity: $r^2 = 0.98$). The linear fit to [Al] suggests that the increase in $N_c$ is due to chain transfer to aluminium.

However, this is accompanied by an *increase* in $M_n$ per chain, and so increased aluminium must additionally accelerate propagation rate in some way. This is perhaps related to the coordination (**Z**) or reaction (**Z***) of the aluminium species with the pendant enamine of the enamine-diimine ligands in **I** and **II** (scheme 2). Therefore, even as chain transfer to Al occurred, propagation rate and $M_n$ increased, since a parallel effect of increasing Al is to increase the potency of active sites. No such clearly linear relationship was identified in the previously studied β-triketimines.[7] However, further increase in Al:Co to 400:1 led to a decrease in both the activity and the molecular weight (76.8% conversion and $3.7 \times 10^5$ g mol$^{-1}$) indicating deactivation of the active centre and further increase in chain transfer to Al.[55] In contrast, in the case of **II**, the activity decreased as the Al/Co increased. The highest activity (100% conversion) was obtained when the ratio was 25:1, with high molecular weight (7.8 x $10^5$ g/mol) due to full conversion increasing the probability of chain transfer to polymer (crosslinking). The activity dropped to 64.7% conversion with lower molecular weight (2.3 x $10^5$ g/mol) as the ratio increased to 150:1. This is more normally expected behavior, where catalyst deactivation and chain transfer both increase at high aluminium concentration.

**Table 4** The effect of DEAC ratio on the polymerization of isoprene by **I** and **II**. [a]

| Catalyst | Al/Co | Time | Conversion (%) | $M_w$[b] (g mol$^{-1}$) ×10$^5$ | $M_n$[b] (g mol$^{-1}$) ×10$^5$ | $Đ$[b] | Microstructure[c] (%) | | | |
|---|---|---|---|---|---|---|---|---|---|---|
| | | | | | | | *Cis*-1,4 | *Trans*-1,4 | 1,2 | 3,4 |
| **I** | 25 | 20 min | 26.8 | 2.8 | 1.4 | 2.00 | 78.7 | 0.9 | 0 | 20.4 |
| | 50 | 20 min | 35.9 | 3.0 | 1.5 | 2.00 | 78.9 | 0.6 | 0 | 20.5 |
| | 100 | 20 min | 50.0 | 3.6 | 1.6 | 2.25 | 78.4 | 0.3 | 0 | 21.3 |
| | 150 | 20 min | 76.0 | 3.8 | 1.7 | 2.24 | 78.2 | 0.2 | 0 | 21.6 |
| | 200 | 20 min | 93.8 | 4.5 | 1.6 | 2.81 | 78.1 | 0 | 0 | 21.9 |
| | 400 | 20 min | 76.8 | 3.8 | 1.4 | 2.71 | 78.5 | 0 | 0 | 21.5 |

Dalton Transactions Accepted Manuscript


This journal is © The Royal Society of Chemistry

| | | | | | | | | | | |
|---|---|---|---|---|---|---|---|---|---|---|
| **II** | 25 | 6 h | 100 | 7.8 | 1.9 | 4.11 | 76.9 | 0.1 | 0 | 23.0 |
| | 50 | 6 h | 90.5 | 3.7 | 1.0 | 3.70 | 79.4 | 0 | 0 | 20.6 |
| | 100 | 6 h | 69.4 | 2.4 | 0.8 | 3.00 | 79.9 | 0.1 | 0 | 20.0 |
| | 150 | 6 h | 64.7 | 2.3 | 0.8 | 2.88 | 79.3 | 0.2 | 0 | 20.5 |

[a] Conditions: Catalyst: 5 µmol; isoprene: 5 mL; solvent: 30 mL chlorobenzene. [b] Determined by GPC. [c] Determined by $^{13}$C NMR.

The type of alkylation reagent was found to play an important role in terms of activity and the results are summarised in Table 5. These catalysts were active only with the alkyl aluminium chlorides: diethylaluminum chloride (DEAC) and ethylaluminum sesquichloride (EASC). They were totally inactive with chloride-free alkyl aluminium co-catalysts such as methylaluminoxane (MAO), trimethyl aluminium (TMA), triethyl aluminium (TEA) and tri-isobutyl aluminium (TIBA). The same behaviour was reported with cobalt complexes **III**.[7] The dependence on chloride has been observed previously in this area: *bis*(N-arylcarboximidoylchloride)-pyridine cobalt(II) complexes behaved similarly in the polymerization of 1,3-butadiene.[56] This phenomenon might relate to the Lewis acidity of the alkylation reagent. Although EASC/**I** was more active (100% conversion) compared to DEAC/**I** (52.9% conversion) under the same conditions, the molecular weight of the produced polymer was lower ($4.0 \times 10^4$ g mol$^{-1}$) and the molecular weight distribution was much higher. This is shown in Figure 5.

The high molecular weight tail may be due to the commencement of chain-transfer to polymer, since the higher activity of **I**/EASC meant that full conversion was reached much earlier. Also, it seems likely on the basis of the lower molecular weights that chain transfer to Al is faster for EASC than for DEAC. Further data and discussion of molecular weight distributions is to be found in supplementary information. The microstructure of the polymer was only slightly affected by the type of co-catalyst. EASC/**I** produced polyisoprene with the higher 1,4-enchainment (82.3%) whereas DEAC/**I** produced 78.4% 1,4-enchainment. Analogous behaviour was observed with 2-(benzimidazolyl)-6-(1-(arylimino)ethyl)pyridine cobalt (II)[20, 57] and ([ArN=C(Me)-(Me)C=NAr]$CoCl_2$)[58] in diene polymerizations.

In the case of **II**, the same patterns were observed: EASC/**II** was more active than DEAC/**II** (100% and 19.0 % conversion respectively) while the molecular weight was around four times lower for EASC/**II** ($2.0 \times 10^4$ g mol$^{-1}$) compared to DEAC/**II** ($8.0 \times 10^4$ g mol$^{-1}$). This huge difference in the molecular weight is mainly ascribed to the differences in active sites. Though the active cations are identical, as mentioned earlier, there are different counter-ions in **I** and **II**, with **II** offering a range of possible aluminium-centred anions, resulting in a range of rates of polymerization.

The dispersities are broader for EASC since the greater activity resulted in earlier full conversion, a situation which encouraged crosslinking (see supplementary data), since the possibility of chain transfer to polymer is increased. Also, EASC is more Lewis-acidic than DEAC. This increases the chance of chain transfer to Al. Therefore, some very high values of dispersity (14) are due to the all of these contributing factors. However, EASC/**II** produced the polymer with the highest level of 1,4-enchainment (82.4%) whereas DEAC/**II** produced 79.5 % 1,4-enchainment. Further investigation of chain transfer due to Al ratio is reported and discussed in supplementary information.

**Table 5** The effect of various alkylation reagents on the polymerization of isoprene by **I** and **II**.[a]

| Catalyst | Al | Time | Conversion (%) | $M_w$[b] (g mol$^{-1}$) ×10$^5$ | $M_n$[b] (g mol$^{-1}$) ×10$^5$ | $Đ$[b] | Microstructure[c] (%) | | | |
|---|---|---|---|---|---|---|---|---|---|---|
| | | | | | | | *Cis*-1,4 | *Trans*-1,4 | 1,2 | 3,4 |
| **I** | DEAC | 10 min | 52.9 | 2.9 | 1.5 | 1.93 | 78.2 | 0.2 | 0 | 21.6 |
| **I** | EASC | 1 min | 100 | 2.0 | 0.4 | 5.0 | 81.6 | 0.7 | 0 | 17.8 |
| **II** | DEAC | 1 h | 19.0 | 1.9 | 0.8 | 2.38 | 79.3 | 0.2 | 0 | 20.5 |
| **II** | EASC | 1 h | 97.3 | 2.8 | 0.2 | 14.0 | 81.3 | 1.1 | 0 | 17.6 |

[a] Conditions: Catalyst: 5 µmol; isoprene: 5 mL; Al/Co: 150; solvent: 30 mL chlorobenzene. [b] Determined by GPC. [c] Determined by $^{13}$C NMR.

Dalton Transactions Accepted Manuscript

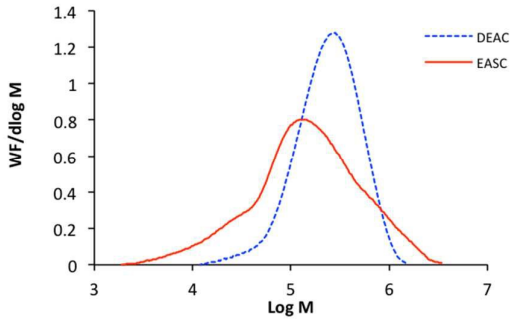


**Figure 5** GPC curves of polyisoprene produced by **I**/DEAC and **I**/EASC systems.

### Catalyst performance comparison

The activity of **I**/EASC, at 6.0 × $10^5$ mol IP $mol^{-1}$Co $h^{-1}$ was much higher than that of **II**/EASC, at 9.7 × $10^3$ mol IP $mol^{-1}$Co $h^{-1}$. Thus, the large, weakly nucleophilic BArF anion was greatly advantageous to activity, as has been found in other polymerization contexts.[59] Furthermore, the best activity of **I** not only was higher than all other Co complexes such as $Co[O_2CCHEt(CH_2)_3CH_3]_2$/DEAC,[46] $[(Ph_2RP)_2CoCl_2]$/MAO,[47, 60] and 2-(N-Et-benzimidazolyl)-6-(1-2,6-dimethylphenyl)ethyl)pyridine$CoCl_2$/EASC,[20, 57] but also higher than the best examples from the lanthanides, as shown in Table 6. The most productive reported lanthanide catalysts, Nd amido complexes activated with aluminium and borane co-catalysts, gave activities of 6 x $10^4$ mol IP $mol^{-1}$Nd $h^{-1}$.[40] In addition, other Co complexes had a range of selectivities with a mixture of the main types of enchainments (e.g. 3,4/*cis*-1,4/*trans*-1,4 of 46/43/9%)[46], (3.4/*cis*-1,4 of 57%/43%)[41] and (*alt*-3,4/1,4-*cis*) [47, 60] while He Sun and co-workers claimed higher *cis*-1,4 (> 94%) than **I** but with much lower activity.[20, 57] While **I**/EASC was ten-fold more active than the best Nd catalyst, *cis*-1,4 selectivities of 82% were lower than the 96% attained with Nd, as shown in Table 6. In wider context, **I**/EASC hugely outperforms almost all other metal complexes such as those of Ni,[61] Ti,[62] Fe,[63, 64] Cr,[51, 65] Y[53, 66, 67] and Nd[48, 68, 69] but there are some complexes more active: for example, the activity of $(Bipy)_2FeCl_2$/MAO [70] was 8.0 × $10^5$ mol IP $mol^{-1}$Co $h^{-1}$, but the produced polymer was mainly atactic 3,4 (67%) with poor selectivity as shown in Table 6. In the case of the aforementioned $[Nd(N(SiMe_3)_2)_3]/B(C_6F_5)_3/{}^iBu_3Al$ system,[40] the activity was 60,188 mol IP $mol^{-1}$Co $h^{-1}$ indicating that it was more active than **I**/DEAC but less active than **I**/EASC . The selectivity of Nd was higher than that of **I** and the produced polymer was mainly *cis*-1,4 with narrow dispersity $Đ$ = 1.53) but the molecular weight was rather low ($M_n$ = 1.34 × $10^3$ g $mol^{-1}$). Though the polymer produced by **I** had a 3,4-content of *ca.* 20%, this is considered as an advantage in some industrial applications where the curing procedure (crosslinking) is facilitated by the presence of alkenyl side-group resulting in good mechanical properties, such as low rolling resistance and/or good skid resistance.[51,5]

**Table 6** A comparison of activities and selectivities of a range of catalysts of isoprene polymerization.

| Catalytic system | Rate<br>mol IP $mol^{-1}$ Metal $h^{-1}$ | Main<br>Selectivity | Other isomers | Notes | Ref |
|---|---|---|---|---|---|
| **I**/ EASC | 6.0 × $10^5$ | *cis*-1,4 (82%) | *trans*-1,4(17.8%)<br>3,4(0.7%) | 1 min, 35 °C, (100% conv.)<br>$M_n$ = 4.0 × $10^4$, $Đ$ = 5 | This work |
| **II**/ EASC | 9.7 × $10^3$ | *cis*-1,4 (81%) | *trans*-1,4 (17.6%)<br>3,4(1.1%) | 1 h, 35 °C, (97.4% conv.)<br>$M_n$ = 2.0 × $10^4$, $Đ$ = 14 | This work |
| 2-(N-Et-benzimidazolyl)-6-(1-2,6-dimethylphenyl)ethyl)pyridine**Co**$Cl_2$/EASC | 5.1 × $10^4$ | *cis*-1,4 (94%) | 3,4 (6%) | > 0.5 h, 30 °C, (51% conv.)<br>$M_n$ = 1.6 × $10^4$. $Đ$ = 2.57 | 20, 57 |
| [**Nd**{$N(SiMe_3)_2$}$_3$]/$B(C_6F_5)_3/{}^iBu_3Al$ | 6.0 × $10^4$ | *cis*-1,4 (96%) | 3,4 (4%) | 2 min, 25°C, (67% conv.)<br>$M_n$ = 1.34 × $10^5$, $Đ$ = 1.53 | 40 |
| $[(Ph_2{}^iPrP)_2$**Co**$Cl_2]$/MAO | 200 | 3,4 (57%) | *cis*-1,4 (43%) | 5 h, 20 °C, (100% conv.)<br>$M_n$ = 3.7 × $10^4$, $Đ$ = 1.9 | 41 |
| **Co**$[O_2CCHEt(CH_2)_3CH_3]_2$/DEAC | 1.44× $10^4$ | 3,4 (46%) | *cis*-1,4 (43%)<br>*trans*-1,4 (9%) | 2 h, 20 °C, (100% conv.) | 46 |
| $[(Ph_2RP)_2$**Co**$Cl_2]$/MAO | 200 | 3,4 (57%) | *cis*-1,4 (43%) | 5 h, 20 °C, (100% conv.)<br>$M_n$ = 3.7 × $10^4$, $Đ$ = 1.9 | 47, 60 |
| $(Bipy)_2$**Fe**$Cl_2$/MAO | 8 × $10^5$ | 3,4 (67%) | *cis*-1,4 (33%) | > 30 s, 20 °C, (100% conv.)<br>$M_n$ = 1.4 × $10^6$, $Đ$ = 1.3. | 70 |

## Conclusion

Dalton Transactions Accepted Manuscript


This journal is © The Royal Society of Chemistry

Novel cationic and neutral enamine-diimine cobalt complexes were synthesised and then fully characterized by elemental analysis, MALDI-MS, IR spectroscopy and single crystal X-ray diffraction. Study of the performance of these complexes in isoprene polymerization showed that **I** was more active than **II**. EASC produced the most active co-catalyst system for both **I** and **II**, but the produced polymer had broader dispersity and lower molecular weight, due to the higher number of active centres and higher rate of chain transfer to aluminium compared to DEAC. The microstructure of polyisoprene was not influenced by the nature of counter-ion at 35 °C; the produced polyisoprene contained a mixture of *cis*-1,4 (up to 80%), *trans*-1,4 and 3,4-enchained monomers at similar levels for both **I** and **II**. However, when temperature was lowered to 20 ˚C, a counter-ion influence was discernible: for **I** both *cis*-1,4 content and activity decreased with reduction in temperature, whereas for **II** only the activity decreased. Further anion effects were noted in response to variation in Al/Co molar ratio. Increasing the Al:Co ratio increased the activity for **I** but decreased it for **II**. All such factors were explainable in terms of ion-pairing effects. In a comparison with a range of other complexes, **I** was found to be the most active of all catalysts in any way selective for *cis*-1,4 polyisoprene (*ca.* 80% selective). The 20% 3,4-content of the polyisoprene provides a potential industrial advantage in providing crosslinking sites in order to improve the mechanical properties of the final products.

## Experimental Section

### General considerations

All procedures were carried out under an atmosphere of nitrogen and the ligands, $CoBr_2$ and NaBArF were stored in a glovebox before they were transferred into the Schlenk tube. Nitrogen gas was dried by passage through a column of phosphorus pentoxide supported on vermiculite. The solvents hexane and tetrahydrofuran (THF) were distilled from sodium/benzophenone, while dichloromethane (DCM) and chlorobenzene were distilled from calcium hydride. Isoprene, $CoBr_2$, diethylaluminum chloride, tri-methyl aluminium, tri-ethyl aluminium, tri-isobutyl aluminium and methylaluminoxane were purchased from Sigma-Aldrich while ethylaluminum sesquichloride was purchased from Acros Organics. NaBArF,[21, 71] and the ligand (L)[23] were synthesised according to literature procedures. A Bruker 500 MHz spectrometer was used in order to record the NMR spectra, using $CDCl_3$ as solvent. Infrared spectra were recorded on a Bruker Alpha-p spectrometer, using OPUS 6.5 software. The mass spectra were recorded using the MALDI technique, with acetonitrile as solvent. Gel permeation chromatography (GPC) was used to measure $M_n$, $M_w$ and $Đ$. GPC was carried out at 35 °C using a PL 2MB500A column in THF at a flow rate of 1 $cm^3$ $min^{-1}$;100 µl was injected using a Viscotek VE2001 GPC equipped with a Viscotek VE3580 Refractive Index detector. X-ray diffraction (XRD) was carried out to measure the structure of single crystals. The data of **I** and **II** was collected on Super Nova diffractometer with Mo K-alpha X-ray source (λ = 0.71073 Å) at 150 K. The collected data were solved using the SUPERFLIP[72] program and refined by the SHELX-97[73] and OLEX2[74] programs.

### Synthesis and characterization of β-tri-ketimine cobalt complexes

**$[(LCo\text{-}\mu\text{-}Br)_2][BArF]_2$ (I)**: A mixture of the ligand (0.22 g, 0.446 mmol), $CoBr_2$ (0.098 g, 0.446 mmol) and NaBArF (0.4 g, 0.450 mmol) was added to a Schlenk tube in a glovebox. THF (20 $cm^3$) was added to the mixture, forming a green solution which was left stirring overnight at room temperature under nitrogen. The THF was then removed, DCM (20 $cm^3$) was added and the solution was filtered through celite under nitrogen. The celite pad was washed with DCM (2×10 $cm^3$) and the filtrate was reduced in volume by 80% under vacuum. The solution was then layered with hexane (50 $cm^3$) and left overnight. Green crystals were formed (0.59 g, 84.4%), mp: 179 °C. Elemental analysis, calculated for $C_{70}H_{63}N_3OF_{24}BCoBr$ (%): C, 53.62; H, 4.05; N, 2.68; Co, 3.76; Br, 5.10. Found: C, 53.47; H, 3.64; N, 2.68; Co, 3.40; Br, 5.47. MS (MALDI) *m/z*: 630.7-633.7 $[(L^3)CoBr]^+$. IR ($cm^{-1}$): 3375 (N-H), 3002-2811 (C-H), 1610 (C=N).

**$[L\text{-}CoBr_2]$ (II):** A mixture of the ligand (0.15 g/ 0.3 mmol) and $CoBr_2$ (0.0664 g/ 0.3 mmol) was transferred into a Schlenk tube in a glovebox. To the mixture, DCM (20 $cm^3$) was added and the solution was stirred and heated to reflux for five hours under nitrogen. The light green solution became dark green over this period. Subsequently, the solvent volume was reduced by 50% and then layered with hexane. Dark turquoise needle crystals were formed. These were recrystallized from *ortho*-dichlorobenzene and hexane, whereupon dark green crystals were obtained (0.12 g/ 56.1%), mp: 220 °C. Elemental analysis, calculated for $C_{34}H_{43}N_3CoBr_2$ (%): C, 57.32; H, 6.08; N, 5.90; Co, 8.27; Br, 22.43. Found: C, 56.47; H, 5.98; N, 5.74; Co, 7.82; Br, 22.24. MS (MALDI) *m/z*: 631.5-634.5 $[(L)CoBr]^+$. IR ($cm^{-1}$): 3411 (N-H), 3020-2800 (C-H), 1628 (C=N).

### Polymerization of isoprene

In a glovebox, the desired amount of catalyst was transferred into a Schlenk tube, to which 30 $cm^3$ of the solvent (chlorobenzene) was added after removal from the glovebox and attachment to a $N_2$/vacuum double manifold. Due to the low boilling point of isoprene, it was required to use a condenser, so a two neck round bottom flask was connected to a condenser which was attached to a $N_2$/vacuum double manifold. When the desired concentration of the catalyst (5 µmol) was added, the desired amount of the alkylating reagent (EASC or $Et_2AlCl$) was added and then the solution was left stirring for five minutes. After that, isoprene (5 $cm^3$, 0.05 mol) was added and then the polymerization was carried out for different times. The polymerization was terminated by pouring the polymerization solution into acidified methanol containing 2,6-di-tert-butyl-4-methylphenol as antioxidant. The solution

Dalton Transactions Accepted Manuscript

was left stirring 12 hours. The polymer was filtered, washed with methanol and then dried under vacuum for 24 hours at room temperature.

## Acknowledgements

The King Abdulaziz City for Science and Technology (KACST) is acknowledged for provision of a studentship to MNA. We would like to thank Dr Eufemio Moreno for his assistance in X-ray data collection and solution. Mr Martin Jennings of the University of Manchester School of Chemistry Analytical Service is acknowledged for provision of elemental analyses. Mr Gareth Smith is gratefully acknowledged for provision of mass spectrometry.

## References

1. R. Cariou, J. J. Chirinos, V. C. Gibson, G. Jacobsen, A. K. Tomov, G. J. P. Britovsek and A. J. P. White, *Dalton Trans.*, 2010, **39**, 9039.
2. S. K. H. Thiele and D. R. Wilson, *J. Macromol. Sci., Polym. Rev.*, 2003, **C43**, 581.
3. J. S. Kim, D. Chandran, D.-W. Park, C.-S. Ha and I. Kim, *Stud. Surf. Sci. Catal.*, 2007, **172**, 525.
4. S. Kaita, M. Yamanaka, A. C. Horiuchi and Y. Wakatsuki, *Macromolecules*, 2006, **39**, 1359.
5. M. J. Vitorino, P. Zinck and M. Visseaux, *Eur. Polym. J.*, 2012, **48**, 1289.
6. G. Viola, F. Bacchelli and S. Valenti, EP1650227A2, 2006.
7. M. N. Alnajrani and F. S. Mair, *RSC Advances*, 2015, **5**, 46372.
8. G. Ricci, A. Forni, A. Boglia and T. Motta, *J. Mol. Catal. A: Chem.*, 2005, **226**, 235.
9. G. Ricci, A. Sommazzi, F. Masi, M. Ricci, A. Boglia and G. Leone, *Coord. Chem. Rev.*, 2010, **254**, 661.
10. D. Gong, B. Wang, H. Cai, X. Zhang and L. Jiang, *J. Organomet. Chem.*, 2011, **696**, 1584.
11. P. Ai, L. Chen, Y. Guo, S. Jie and B.-G. Li, *J. Organomet. Chem.*, 2012, **705**, 51.
12. D. Gong, B. Wang, X. Jia and X. Zhang, *Dalton Trans.*, 2014, **43**, 4169.
13. L. Porri, A. Giarrusso and G. Ricci, *Prog. Polym. Sci.*, 1991, **16**, 405.
14. H. Liu, X. Jia, F. Wang, Q. Dai, B. Wang, J. Bi, C. Zhang, L. Zhao, C. Bai, Y. Hu and X. Zhang, *Dalton Trans.*, 2013, **42**, 13723.
15. D. Gong, X. Jia, B. Wang, X. Zhang and L. Jiang, *J. Organomet. Chem.*, 2012, **702**, 10.
16. D. Gong, X. Jia, B. Wang, F. Wang, C. Zhang, X. Zhang, L. Jiang and W. Dong, *Inorg. Chim. Acta*, 2011, **373**, 47.
17. G. B. Brook and E. A. Brandes *Smithells Light Metals Handbook*, Elsevier Science, Burlington, 1998.
18. V. Appukuttan, L. Zhang, J. Y. Ha, D. Chandran, B. K. Bahuleyan, C.-S. Ha and I. Kim, *J. Mol. Catal. A: Chem.*, 2010, **325**, 84.
19. V. Appukuttan, L. Zhang, C.-S. Ha and I. Kim, *Polymer*, 2009, **50**, 1150.
20. G. Wang, X. Jiang, W. Zhao, W.-H. Sun, W. Yao and A. He, *J. Appl. Polym. Sci.*, 2014, **131**, 39703.
21. D. Barnes, G. L. Brown, M. Brownhill, I. German, C. J. Herbert, A. Jolleys, A. R. Kennedy, B. Liu, K. McBride, F. S. Mair, R. G. Pritchard, A. Sanders and J. E. Warren, *Eur. J. Inorg. Chem.*, 2009, 1219.
22. J. Cullinane, A. Jolleys and F. S. Mair, *Dalton Trans.*, 2013, **42**, 11971.
23. N. G. Hamedani, H. Arabi, G. H. Zohuri, F. S. Mair and A. Jolleys, *J. Polym Sci. A. Polym. Chem*, 2013, **51**, 1520.
24. M. N. Alnajrani and F. S. Mair, *Dalton Trans.*, 2014, **43**, 15727.
25. P. T. Anastas and J. C. Warner, *Green chemistry : theory and practice*, Oxford University Press, Oxford, UK, 1998.
26. R. Shannon, *Acta Crystallographica Section A*, 1976, **32**, 751.
27. S.-J. Song, T.-F. Xiao, C. Redshaw, X. Hao, F.-S. Wang and W.-H. Sun, *J. Organomet. Chem.*, 2011, **696**, 2594.
28. V. Rosa, S. A. Carabineiro, T. Aviles, P. T. Gomes, R. Welter, J. M. Campos and M. R. Ribeiro, *J. Organomet. Chem.*, 2008, **693**, 769.
29. T. V. Laine, M. Klinga, A. Maaninen, E. Aitola and M. Leskela, *Acta Chem. Scand.*, 1999, **53**, 968.
30. M. Tanabiki, Y. Sunada and H. Nagashima, *Organometallics*, 2007, **26**, 6055.
31. J. Feldman, S. J. McLain, A. Parthasarathy, W. J. Marshall, J. C. Calabrese and S. D. Arthur, *Organometallics*, 1997, **16**, 1514.
32. E. K. Cope-Eatough, F. S. Mair, R. G. Pritchard, J. E. Warren and R. J. Woods, *Polyhedron*, 2003, **22**, 1447.
33. J. M. Stauber, A. L. Wadler, C. E. Moore, A. L. Rheingold and J. S. Figueroa, *Inorg. Chem.*, 2011, **50**, 7309.
34. J. D. Azoulay, Z. A. Koretz, G. Wu and G. C. Bazan, *Angew. Chem., Int. Ed.*, 2010, **49**, 7890.
35. C. Cui, H. Hao, M. Noltemeyer, H.-G. Schmidt and H. W. Roesky, *Polyhedron*, 2000, **19**, 471.
36. S. Tobisch, *Can. J. Chem.*, 2009, **87**, 1392.
37. L. Perrin, F. Bonnet, M. Visseaux and L. Maron, *Chem. Commun.*, 2010, **46**, 2965.
38. X. Kang, Y. Luo, G. Zhou, X. Wang, X. Yu, Z. Hou and J. Qu, *Macromolecules*, 2014, **47**, 4596.
39. G. Lanza, I. L. Fragala and T. J. Marks, *J. Am. Chem. Soc.*, 1998, **120**, 8257.
40. N. Martins, F. Bonnet and M. Visseaux, *Polymer*, 2014, **55**, 5013.
41. D. G. Boucher, I. W. Parsons and R. N. Haward, *Makromol. Chem.*, 1974, **175**, 3461.
42. L. Deng, T. K. Woo, L. Cavallo, P. M. Margl and T. Ziegler, *J. Am. Chem. Soc.*, 1997, **119**, 6177.
43. P. J. Flory, *J. Am. Chem. Soc.*, 1947, **69**, 2893.
44. S. Jie, P. Ai and B.-G. Li, *Dalton Trans.*, 2011, **40**, 10975.
45. C. Breutel, P. S. Pregosin, R. Salzmann and A. Togni, *J. Am. Chem. Soc.*, 1994, **116**, 4067.
46. V. A. Yakovlev, I. F. Gavrilenko, N. N. Glebova and G. N. Bondarenko, *Polym. Sci., Ser. B*, 2014, **56**, 31.
47. G. Ricci, A. Forni, A. Boglia, T. Motta, G. Zannoni, M. Canetti and F. Bertini, *Macromolecules*, 2005, **38**, 1064.
48. A. Fischbach, M. G. Klimpel, M. Widenmeyer, E. Herdtweck, W. Scherer and R. Anwander, *Angew. Chem., Int. Ed.*, 2004, **43**, 2234.
49. J. Wolpers, H. B. Fuchs, C. Herrmann and W. Hellermann, EP456902A1, 1991.
50. J. D. Massie II, W. L. Hsu, A. F. Halasa and P. H. Sandstrom, US5356997A, 1994.
51. B. Gao, X. Luo, W. Gao, L. Huang, S.-m. Gao, X. Liu, Q. Wu and Y. Mu, *Dalton Trans.*, 2012, **41**, 2755.
52. B. Liu, L. Li, G. Sun, J. Liu, M. Wang, S. Li and D. Cui, *Macromolecules*, 2014, **47**, 4971.

Dalton Transactions Accepted Manuscript

 This journal is © The Royal Society of Chemistry

53. Z. Jian, D. Cui, Z. Hou and X. Li, *Chem. Commun.*, 2010, **46**, 3022.
54. Y. Pan, T. Xu, G.-W. Yang, K. Jin and X.-B. Lu, *Inorg. Chem.*, 2013, **52**, 2802.
55. P. Cass, K. Pratt, T. Mann, B. Laslett, E. Rizzardo and R. Burford, *J. Polym. Sci. Part A: Polym. Chem.*, 1999, **37**, 3277.
56. H. Liu, X. Jia, F. Wang, Q. Dai, B. Wang, J. Bi, C. Zhang, L. Zhao, C. Bai, Y. Hu and X. Zhang, *Dalton Trans.*, 2013, **42**, 13723.
57. A. He, G. Wang, W. Zhao, X. Jiang, W. Yao and W.-H. Sun, *Polym. Int.*, 2013, **62**, 1758.
58. X. Jia, H. Liu, Y. Hu, Q. Dai, J. Bi, C. Bai and X. Zhang, *Chin. J. Cat.*, 2013, **34**, 1560.
59. A. R. O'Connor, P. S. White and M. Brookhart, *J. Am. Chem. Soc.*, 2007, **129**, 4142.
60. G. Ricci, G. Leone, A. Boglia, A. C. Boccia and L. Zetta, *Macromolecules*, 2009, **42**, 9263.
61. U. Gebauer, S. Engelmann and K. Gehrke, *Acta Polym.*, 1989, **40**, 341.
62. W. M. Saltman, W. E. Gibbs and J. Lal, *J. Am. Chem. Soc.*, 1958, **80**, 5615.
63. J. Raynaud, J. Y. Wu and T. Ritter, *Angew. Chem., Int. Ed.*, 2012, **51**, 11805.
64. X. Jiang, X. Wen, W.-H. Sun and A. He, *J. Polym. Sci., Part A: Polym. Chem.*, 2014, **52**, 2395.
65. Z. Liu, W. Gao, X. Liu, X. Luo, D. Cui and Y. Mu, *Organometallics*, 2011, **30**, 752.
66. L. Zhang, Y. Luo and Z. Hou, *J. Am. Chem. Soc.*, 2005, **127**, 14562.
67. L. Zhang, T. Suzuki, Y. Luo, M. Nishiura and Z. Hou, *Angew. Chem., Int. Ed.*, 2007, **46**, 1909.
68. A. Fischbach, F. Perdih, E. Herdtweck and R. Anwander, *Organometallics*, 2006, **25**, 1626.
69. M. Zimmermann, N. A. Froeystein, A. Fischbach, P. Sirsch, H. M. Dietrich, K. W. Toernroos, E. Herdtweck and R. Anwander, *Chem. Eur. J.*, 2007, **13**, 8784.
70. G. Ricci, D. Morganti, A. Sommazzi, R. Santi and F. Masi, *J. Mole. Catal. A: Chem.*, 2003, **204–205**, 287.
71. M. Brookhart, B. Grant and A. F. Volpe, Jr., *Organometallics*, 1992, **11**, 3920.
72. L. Palatinus and G. Chapuis, *J. Appl. Crystallogr.*, 2007, **40**, 786.
73. G. M. Sheldrick, *Acta Crystallogr., Sect. A: Found. Crystallogr.*, 2008, **64**, 112.
74. O. V. Dolomanov, L. J. Bourhis, R. J. Gildea, J. A. K. Howard and H. Puschmann, *J. Appl. Crystallogr.*, 2009, **42**, 339.

Dalton Transactions Accepted Manuscript